

Transient Receptor Potential Vanilloid 4 Deficiency Suppresses Unloading-Induced Bone Loss

FUMITAKA MIZOGUCHI,^{1,2,3} ATSUKO MIZUNO,⁴ TADAYOSHI HAYATA,¹ KAZUHISA NAKASHIMA,^{1,2} STEFAN HELLER,⁵ TAKASHI USHIDA,⁶ MASAHIRO SOKABE,⁷ NOBUYUKI MIYASAKA,^{2,3} MAKOTO SUZUKI,⁴ YOICHI EZURA,^{1,8*} AND MASAKI NODA^{1,2,8,9*}

¹Department of Molecular Pharmacology, Medical Research Institute, Tokyo Medical and Dental University, Tokyo, Japan

²The 21st Century Center of Excellence (COE) Program for Frontier Research on Molecular Destruction and Reconstruction of Tooth and Bone, Tokyo, Japan

³Department of Medicine and Rheumatology, Graduate School, Tokyo Medical and Dental University, Tokyo, Japan

⁴Department of Pharmacology, Division of Molecular Pharmacology, Jichi Medical School, Tochigi, Japan

⁵Department of Otolaryngology, Head and Neck Surgery and Molecular and Cellular Physiology, Stanford University School of Medicine, Stanford, California

⁶Center for Disease Biology and Integrative Medicine School of Medicine, The University of Tokyo, Tokyo, Japan

⁷Department of Physiology, Nagoya University Graduate School of Medicine, Nagoya, Japan

⁸Hard Tissue Genome Research Center, Tokyo Medical and Dental University, Tokyo, Japan

⁹ABJS Strategic Research Network Project in JSPS Core to Core Program

Mechanosensing is one of the crucial components of the biological events. In bone, as observed in unloading-induced osteoporosis in bed ridden patients, mechanical stress determines the levels of bone mass. Many molecules have been suggested to be involved in sensing mechanical stress in bone, while the full pathways for this event has not yet been identified. We examined the role of TRPV4 in unloading-induced bone loss. Hind limb unloading induced osteopenia in wild-type mice. In contrast, TRPV4 deficiency suppressed such unloading-induced bone loss. As underlying mechanism for such effects, TRPV4 deficiency suppressed unloading-induced reduction in the levels of mineral apposition rate and bone formation rate. In these mice, unloading-induced increase in the number of osteoclasts in the primary trabecular bone was suppressed by TRPV4 deficiency. Unloading-induced reduction in the longitudinal length of primary trabecular bone was also suppressed by TRPV4 deficiency. TRPV4 protein is expressed in both osteoblasts and osteoclasts. These results indicated that TRPV4 plays a critical role in unloading-induced bone loss.

J. Cell. Physiol. 216: 47–53, 2008. © 2008 Wiley-Liss, Inc.

Disuse osteoporosis is a critical issue in patients with reduced locomotor function in bed-ridden patients due to cardiovascular, brain and skeletal diseases. In such unloading-induced osteoporosis, loss of mechanical stress has been considered to be responsible for the impairment in the maintenance of bone mass (Ehrlich and Lanyon, 2002). Environmental changes in cells in local milieu are transduced into biochemical signals, which regulate cell growth, differentiation, shape changes, and survival (Vogel and Sheetz, 2006). In bone, unloading suppresses bone formation and activates bone resorption; these phenomena are exerted by many types of bone cells including osteoblast, osteocytes, and osteoclasts. It has been suggested that these cells in bone are in the machineries to sense mechanical stress in this tissue (Liedert et al., 2006; Tatsumi et al., 2007). Candidate molecules sensing mechanical stresses include ion-channels, integrins and cytoskeleton molecules. However, exact molecules involved in these machineries have not been fully understood.

Ion-channels have been extensively investigated, for example, L-type voltage-sensitive calcium channels have been suggested to sense mechanical stress on osteoblasts or osteocytes by *in vitro* studies (Genetos et al., 2005). Also alpha subunit of epithelial sodium channels has been investigated in similar context (Kizer et al., 1997; Pavalko et al., 2003). However, *in vivo* roles of these channels in the maintenance of

bone metabolism have not been clarified. In general, ion-channels translate chemical and physical stimuli applied on cells into electrical or biochemical signals within the cells (Voets

Contract grant sponsor: Japanese Ministry of Education.

Contract grant sponsor: Japan Space Forum.

Contract grant sponsor: JAXA.

Contract grant sponsor: ABJS Strategic Research Network Project in JSPS Core to Core Program.

Contract grant sponsor: 21st Century Center of Excellence (COE) Program for Frontier Research on Molecular Destruction and Reconstitution of Tooth and Bone.

Contract grant numbers: 17012008, 18109011, 18659438, 18123456.

*Correspondence to: Masaki Noda and Yoichi Ezura, Department of Molecular Pharmacology, Medical Research Institute, Tokyo Medical and Dental University, 3-10 Kanda-Surugadai, 2-chome Chiyoda-ku, Tokyo 101-0062, Japan.
E-mail: noda.mph@mri.tmd.ac.jp

Received 25 August 2007; Accepted 21 November 2007

DOI: 10.1002/jcp.21374

and Nilius, 2003), and in most cases, calcium plays roles in the signal transduction. In steady states, intracellular calcium levels are maintained at two to three orders of magnitude lower than those of extracellular space. Upon stimulation, intracellular calcium rapidly increases, in part through calcium influx via the channels across the membrane (Pavalko et al., 2003; Ramsey et al., 2006), and induces diverse cellular responses.

Transient receptor potential channels (TRPs) are a family of channels serving as entry point of physical stimuli in several instances. These stimuli include temperature, touch, pain, and osmolarity (Clapham, 2003). One of the members, transient receptor potential vanilloid 4 (TRPV4) is a calcium permeable nonselective cation channel, and are involved in physical sensing in various types of tissues. For example, in brain and kidney, it is involved in osmotic sensation (Liedtke et al., 2000; Liedtke and Friedman, 2003; Mizuno et al., 2003), and in skin and nervous system it function in temperature sensation (Todaka et al., 2004; Lee et al., 2005). In neurons, it appeared to sense high-threshold heat and pressure (Caterina et al., 1999; Suzuki et al., 2003b). In vitro studies revealed that TRPV4 is activated by diverse ranges of physical signals including fluid shear stress (Gao et al., 2003). These findings led us to hypothesize that TRPV4 would be one of the candidates for the mechano-sensing channels acting in bone tissue.

Mice deficient in TRPV4 were previously generated (Mizuno et al., 2003; Todaka et al., 2004). In these homozygous TRPV4 mutant mice, no apparent bone and growth phenotypes were detected at least through superficial observations. However, possibilities that in certain conditions exposing in abnormal conditions would alter the responses to the mechanical stimuli have not been tested yet. Therefore, in this study, we investigated the effects of hindlimb unloading on the mice deficient in TRPV4 and compared them with wild-type mice. Bone histomorphometric analyses revealed a possible contribution of this molecule to rapid loss of bone mass triggered by continuous loss of mechanical stimuli in vivo.

Materials and Methods

Animals

TRPV4 deficient mice were generated on C57BL/6 background as described previously (Mizuno et al., 2003). To expand the colony, heterozygous TRPV4 deficient mice were crossed, and resultant pairs of homozygous TRPV4 deficient mice, as well as wild-type (WT) mice were sib-mated. These mice were randomly divided into control (loaded) and unloaded (tail-suspension) groups. All animals were housed under controlled conditions at 24°C on a 12-h light and 12-h dark cycle. The experiments were approved by the animal welfare committee of Tokyo Medical and Dental University.

Tail-suspension experiment for hind limb unloading

Total of 27 female mice were used in the experiments. For tail suspension, 14 WT and 13 homozygous TRPV4 deficient mice were divided into two groups and one was subjected to tail suspension and the other was maintained under normal housing condition. Experiments were conducted according to the protocol described previously (Ishijima et al., 2001). Briefly, mice were fed in a normal cage, keeping their hind-limbs avoid to touch bottom of the cage. To keep this stature of mice, one end of a metal clip was attached to the tail using adhesive tape, and the other end of the clip was hooked to an overhead bar. The height of suspension was set to have mice at 30 degrees head down tilt.

Two-dimensional (2D) and three-dimensional (3D) micro X-ray computed tomography (μ CT) analysis

2D- μ CT analysis was conducted on dissected femora, using μ CT equipment, Musashi (Nittetsu ELEX, Kitakyushu, Japan). To

evaluate the thickness of primary trabeculae of distal femur, mid-sagittal images of distal metaphysis were selected in each sample, and the thickness was measured at defined five points distributed across the antero-posterior axis of the femur (see Fig. 2A and the legend). Finally, the averaged value from the five-point measurement per sample was regarded as a parameter for longitudinal length of primary trabecular bone.

3D- μ CT analysis was conducted using an equipment, Scan-Xmate-E090 (Comscan Techno Co., Ltd, Sagamihara, Japan) and a computer software, Tri/3D-Bon (Ratoc System Engineering Co., Ltd, Tokyo, Japan). Bone volume/tissue volume (BV/TV), as well as trabecular number (Tb.N), and other microarchitectural parameters were analyzed in the secondary trabecular regions from 0.2 to 0.76 mm away from the chondroosseous junction.

Bone histomorphometric analysis

Calcein labeling was conducted to estimate the levels of newly formed bone within a unit time period according to the methods described elsewhere (Parfitt et al., 1987; Morinobu et al., 2005). Briefly, calcein (4 mg/kg body weight) was injected intraperitoneally 2 and 4 days before sacrifice. Femora were fixed in 70% ethanol and embedded in glycomethacrylate. Sagittal histological sections were prepared, and the calcein bands were visualized based on confocal laser microscopy with an excitation wavelength of 488 nm and a 550 nm band-pass filter. Single labeled bone surface (sLS), double labeled bone surface (dLS) and total bone surface (BS) were separately measured. Mineralizing surface (MS) per BS was calculated as (dLS + sLS/2)/BS. The distance between the parallel calcein lines was measured to yield mineral apposition rate (MAR (μ m/day)). Bone formation rate (BFR) was calculated as MAR multiplied by (MS/BS). Histomorphometric analysis was performed by focusing on the area of 0.31 mm² (0.56 × 0.56 mm) in the distal end of the femora. In the decalcified section, osteoclast number per bone surface (N.Oc/BS, N/mm) and osteoclast surface per bone surface (Oc.S/BS, %) were analyzed based on tartrate-resistant acid phosphatase (TRAP) staining in sagittal sections of the tibiae. Staining was performed as described previously (Morinobu et al., 2005). TRAP positive cells containing one or more nuclei and sitting on the surface of the trabeculae were identified as osteoclasts. One section per animal was analyzed for these parameters.

Immunohistochemistry

Immunohistochemical analysis was performed on decalcified sections of the femora, using Vecstatine Elite ABC kit (Vector, Burlingame, CA). For staining, sections were deparaffinized and hydrated by serial soak with xylene and ethanol, and then incubated in 0.3% H₂O₂ for 30 min. Sections were blocked by 5% goat serum in PBS for 45 min, and then incubated with polyclonal anti-TRPV4 antibody (Cuajungco et al., 2006) at 1:1,000 dilution, over night at 4°C. After washing in PBS, sections were incubated with 1% biotinylated anti-rabbit IgG antibody for 30 min, and then incubated with Avidin DH and biotinylated horse radish peroxidase for 30 min. After washing, stain was visualized by incubating with 3,3'-Diaminobenzidine, tetra-hydrochloride (DAB) for 5 min. Counter-stained sections with hematoxylin were mounted and underwent for microscopic analysis. Background staining was checked by treating the sections similarly except for the use of first antibody (i.e., secondary antibody alone). This procedure provided no obvious staining (data not shown).

RT-PCR analysis

For RT-PCR analysis, dissected femora were soaked with "RNA later" (Sigma, St. Louis, MO) immediately and frozen at -20°C until use. The tissues were homogenized in Trizol reagent (Invitrogen, Carlsbad, CA), and total RNA was extracted according to the manufacturer's protocol. Reverse transcription (RT) was carried out using 1 μ g total RNA in 20 μ l volume reaction, containing

25 µg/ml Oligo(dT)-primer (Invitrogen), 0.125 mM deoxynucleotide triphosphate mix (TAKARA, Ohtsu, Japan), 10 mM dTT and 200 U of Superscript II reverse transcriptase (Invitrogen). Complementary DNA was amplified in a 25 µl reaction mixture containing 2.5 mM deoxynucleotide triphosphate mix, 10 µM specific primers and 1 unit of rTaq DNA polymerase (Takara). After an initial denaturation at 94°C for 2 min, amplifications were performed at 94°C for 40 sec, 60°C for 1 min, and 72°C for 1 min in a GeneAmp PCR system 9700 (Applied Biosystems, Foster City, CA). The cycle number was determined so that the PCR product levels were within a linear range. Ethidium bromide-stained DNA bands were quantified using an image analyzer Bio-ID System (Vilber Lourmat, Torcy, France). Relative mRNA expressions for genes of interest were calculated by normalizing the obtained band intensities to that of glyceraldehyde-3-phosphate dehydrogenase gene (*GAPDH*). Primer sequences used are as follows; *GAPDH*, forward, 5'-ACC ACA GTC CAT GCC ATC AC-3', and reverse, 5'-TCC ACC ACC CTG TTG CTG TA-3'; *TRPV4*, forward, 5'-TTC ATC AAC TCG CCC TTC AGA G-3', and reverse, 5'-GTT GAG AAC TGT CTC CAG GTT G-3'.

Cell culture

MC3T3-E1 cells were cultured in alpha-minimal essential medium (αMEM) supplemented with 10% fetal bovine serum (FBS). RAW264.7 cells were cultured in Dulbecco's modified eagle's medium supplemented with 10% FBS. For osteoclastogenesis assay, RAW264.7 cells were treated with 100 ng/ml RANKL (R&D, Minneapolis, MN) or control vehicle for 48 h.

Statistical analysis

To test an existence of interactive effects between the loading/unloading status and differences in genotypes on bone response, two-way analysis of variance (2×2 ANOVA) was performed. When interactive effect was judged to be statistically significant, Student's *t*-test was used for comparison of two groups except for trabecular number where Welch's test was used. Difference was judged to be statistically significant when *P* values were less than 0.05. All the numeral data in the results were presented as mean values ± standard deviations (SD).

Results

TRPV4 deficiency suppresses unloading-induced secondary trabecular bone loss

To test the hypothesis that TRPV4 would be involved in the mechanical regulation of bone mass, TRPV4 deficient mice and wild-type (WT) mice were subjected to hind-limb unloading. Base line body weight levels were similar between wild-type and TRPV4 deficient mice. 3D-µCT analysis indicated that unloading caused sparsity in the architecture of the secondary trabecular bone as known before (Fig. 1A, WT, unload). In control (load) TRPV4 deficient mice, µCT pictures revealed pattern of trabecular bone architecture similar to that of control WT mice. In contrast to WT, TRPV4 deficient mice did not reveal any pattern changes induced by hind-limb unloading (Fig. 1A, KO, unload). Quantification of the 3D-bone volume per tissue volume indicated that unloading induced reduction by about 30% ($P < 0.01$) after 2 weeks in WT (Fig. 1B). The base line levels of bone volume in control TRPV4 deficient mice were similar to those in WT mice. Quantification also revealed that TRPV4 deficiency suppressed the unloading-induced reduction in the quantified bone volume (Fig. 1B). Further elemental analysis indicated that the number of trabecular bone was reduced by about 20% ($P < 0.05$) due to unloading in WT mice. TRPV4 deficient mice exhibited similar base line levels of trabecular number compared to WT, and the level of this parameter was not reduced in TRPV4 deficient mice even after

unloading (Fig. 1C). Other micro-architectural parameters tended to show similar trend but the differences were not statistically significant (data not shown). Thus, TRPV4 deficiency preserved bone even after unloading.

TRPV4 deficiency suppresses unloading-induced primary trabecular bone loss

Primary spongiosa region has been analyzed to estimate the changes in bone juxtaposed to growth plate (Miao et al., 2004; Xian et al., 2007, 2008). Hind-limb unloading caused reduction in the longitudinal length (height) of primary trabecular bone columns juxtaposed to the growth plate in WT mice (Fig. 2A,B top parts). The base line height of primary trabecular bone columns juxtaposed to the growth plate in deficient mice was similar to that in WT mice. In contrast to WT mice, TRPV4 deficiency suppressed the loss of the height of the primary trabecular bone column induced by unloading (Fig. 2B bottom parts). Quantification of the changes in the height of primary trabecular bone revealed reduction by about 40% ($P < 0.01$) in WT after unloading, while TRPV4 deficiency suppressed such loss of the height in the primary trabecular bone after unloading (Fig. 2C). Therefore, TRPV4 deficiency suppressed unloading-induced bone loss in both primary and secondary trabecular regions.

TRPV4 deficiency suppressed unloading-induced reduction of bone formation

To further understand the bases for such TRPV4 deficiency-induced suppression of bone loss, we examined the

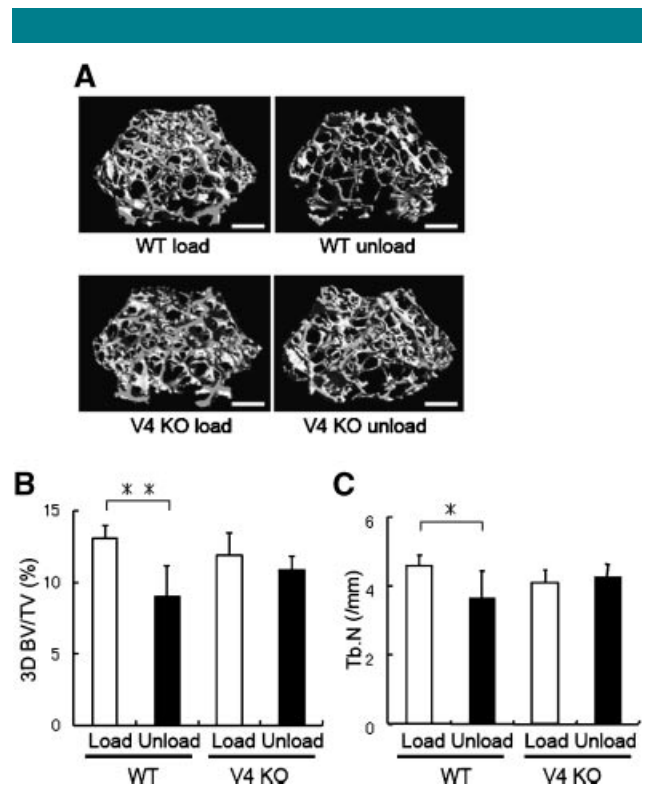


Fig. 1. TRPV4 deficiency suppresses unloading-induced secondary trabecular bone loss. Representative 3-dimensional (3D)-µCT images of the distal metaphyseal regions of femora in loaded and unloaded groups of wild-type (WT) and TRPV4 deficient (V4KO) mice (A). Scale bar indicates 400 µm. B, C: Quantification of the 3D images shown in (A): bone volume/tissue volume (BV/TV) (B), trabecular number (Tb.N) (C). Open and closed bars indicate loaded and unloaded groups respectively (* $P < 0.05$ and ** $P < 0.01$). Six to seven mice were used in each group.

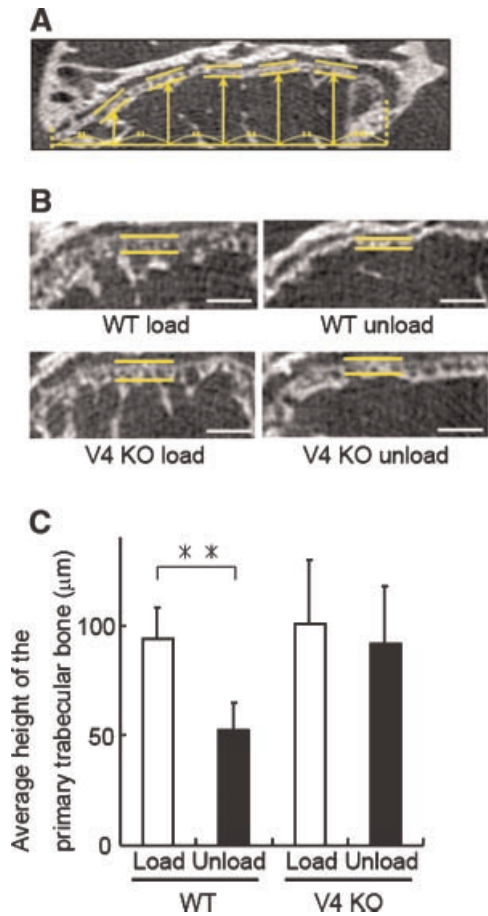


Fig. 2. TRPV4 deficiency suppresses unloading-induced primary trabecular bone loss. Longitudinal length of primary trabecular bone was quantified based on measurement at five separate points as indicated in the μ CT image shown in (A). Sagittal sections of the femora were used. Representative images of the primary trabecular bone of each group are shown (B). The distance between the parallel lines indicate the height of the primary trabecular bone (B). Unloading reduced the longitudinal length of primary trabecular bone in wild-type mice (WT), while such reduction was not observed in TRPV4 deficient mice (V4KO) (B,C) (** $P < 0.01$). Six to seven mice were used per each group. Scale bar indicates 200 μ m. [Color figure can be viewed in the online issue, which is available at www.interscience.wiley.com.]

dynamic bone formation parameters based on the analysis of calcein double-labeling as described in Materials and Methods Section (Fig. 3A). This analysis provides in vivo estimation of osteoblastic activity with respect to accumulation of bone mass. Mineral apposition rate (MAR) was reduced by about 30% ($P < 0.05$) due to unloading in WT. TRPV4 deficiency did not alter the baseline levels of MAR, however it suppressed the reduction in MAR levels induced by unloading (Fig. 3B). Bone formation rate (BFR) was reduced by about 50% ($P < 0.01$) due to unloading in WT. TRPV4 deficiency per se did not alter the levels of BFR in loaded condition. In contrast to WT, TRPV4 deficiency suppressed the decrease in BFR induced by unloading (Fig. 3C). Mineralizing surface analysis did not reveal statistically significant differences among the groups (data not shown). These data indicate that though TRPV4 is not involved in the maintenance of base line bone mass, at least one of the targets of TRPV4 action during the changes caused by mechanical stimuli is bone formation.

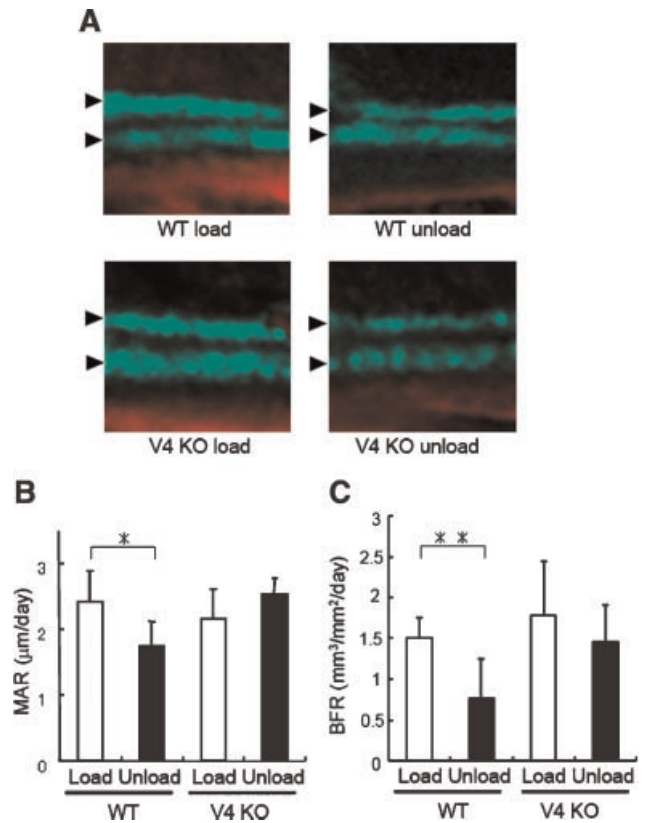


Fig. 3. TRPV4 deficiency suppressed unloading-induced reduction of bone formation. Bone formation activity was evaluated in vivo as described in Materials and Methods Section. Calcein bands were visualized to obtain dynamic histomorphometric parameters. Representative images from each group are shown (A). Unloading-induced decrease in the levels of mineral apposition rate (MAR) (B) and bone formation rate (BFR) (C) in wild-type mice (WT) was not observed in TRPV4 deficient mice (V4 KO) (* $P < 0.05$ and ** $P < 0.01$). Six to seven mice per each group were used. [Color figure can be viewed in the online issue, which is available at www.interscience.wiley.com.]

TRPV4 deficiency suppressed unloading-induced increase of osteoclasts in primary trabecular bone

Since bone mass levels are determined by bone formation as well as bone resorption activities, we examined the effects of TRPV4 deficiency on bone resorption in these mice. Quantification of TRAP positive cells at the primary trabecular regions indicated unloading-induced increase by about 30% ($P < 0.05$) in the number of TRAP positive cells in WT (Fig. 4A,B). TRPV4 deficiency per se did not alter TRAP positive cell number in the control loaded mice (Fig. 4B). In contrast to WT, TRPV4 deficiency suppressed unloading-induced increase in the number of TRAP positive cells in the primary trabecular regions (Fig. 4B). Unloading induced increase by about 50% ($P < 0.01$) in the osteoclast surface at the primary trabecular regions and TRPV4 deficiency also suppressed such alteration due to unloading (Fig. 4C). In the secondary trabecular bone, osteoclast number and osteoclast surface were not significantly altered by unloading in WT or TRPV4 deficient mice (data not shown). Thus, TRPV4 is involved in the unloading-induced regulation of osteoclastic activity in the primary trabecular region.

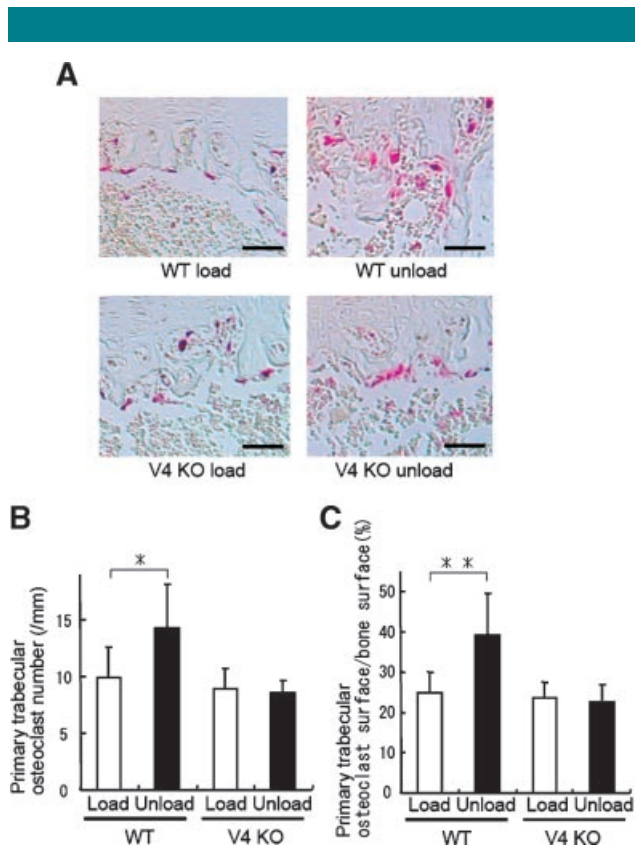


Fig. 4. TRPV4 deficiency suppressed unloading-induced increase of osteoclasts in primary trabecular bone. Primary trabecular regions of the epiphyses of tibiae were examined for osteoclasts based on TRAP staining (magnification 200 \times : A). Scale bar indicates 50 μ m. Unloading-induced increase in the levels of N.Oc/BS (B) and Oc.S/BS (C) was not observed in TRPV4 deficient mice (* $P < 0.05$, ** $P < 0.01$). Six to seven mice per group were used.

TRPV4 is expressed in osteoblasts and osteoclasts

We further addressed whether TRPV4 per se is expressed in bone. For this, we examined mRNA expression in the femora. In the mRNA pool prepared from whole bone (femur), we detected TRPV4 at relatively high levels (Fig. 5A). TRPV4 expression levels in the metaphyseal/epiphyseal regions were close to those in the whole bone (Fig. 5A). However, in the bone marrow regions, the levels were low. In the cortical bone regions, intermediate levels of expression of TRPV4 were observed (Fig. 5A). We also asked whether TRPV4 is expressed in osteoblasts or osteoclasts. In order to address this point, we examined the TRPV4 expression immunohistologically. TRPV4 signals were positive in the osteoblastic cells lining on the endosteal surface of the bone (Fig. 5B). TRPV4 signals of osteocytes embedded in bone were less obvious (Fig. 5B). Osteoclasts in the primary trabecular regions were also positive for TRPV4 signals (Fig. 5C). We also tested whether TRPV4 is expressed in the osteoblastic cell lines. MC3T3-E1 cells are derived from murine calvarial bone and express osteoblastic marker genes (Sudo et al., 1983). In these cells, TRPV4 was expressed at relatively high levels (Fig. 5D). RAW264.7 cells differentiate into osteoclast like cells upon the treatment with RANKL (Hsu et al., 1999). TRPV4 mRNA levels were detected in the baseline condition in these cells and the levels of TRPV4 expression were increased about twofold ($P < 0.01$) by the treatment with RANKL (Fig. 5D) in association with the morphological differentiation of these cells into osteoclast like cells (data not shown). Thus, TRPV4 is

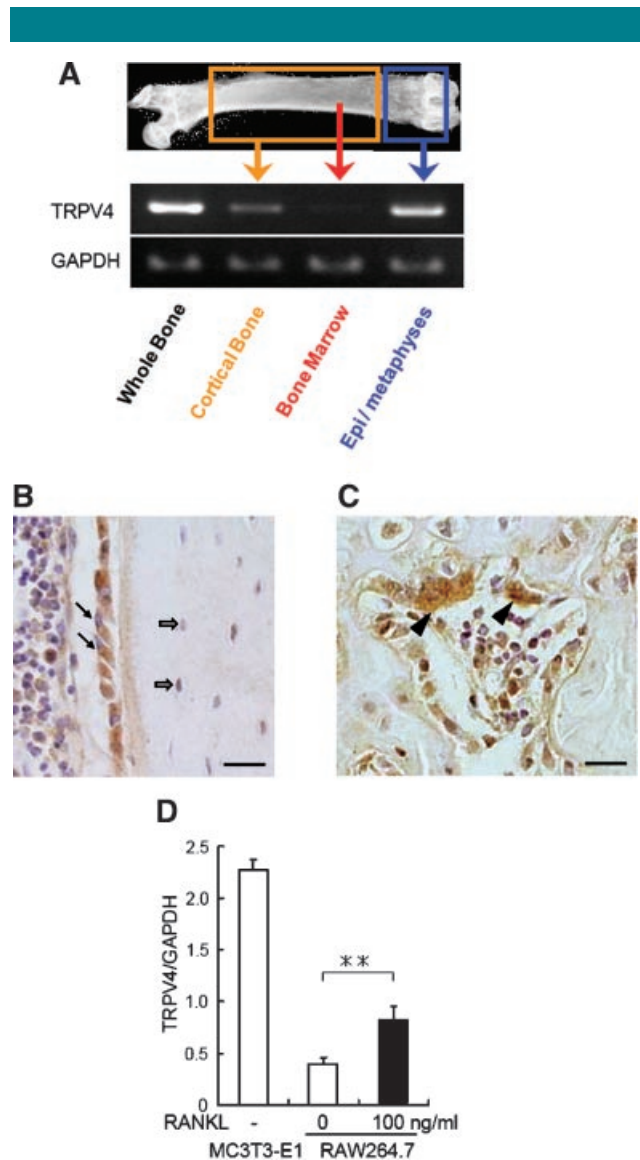


Fig. 5. TRPV4 is expressed in osteoblasts and osteoclasts. RNA was prepared from femora of mice and was subjected to RT-PCR analysis. Femora were either used as a whole bone or were divided into the three regions including epi/metaphyseal (blue rectangle), cortical (orange rectangle) and bone marrow (red arrow) compartments (A, upper part). TRPV4 mRNA was expressed in epi/metaphyseal region (blue) at the levels similar to those in whole bone, while expression of TRPV4 mRNA in cortical (orange) or bone marrow (red) region was less compared to other regions (A, lower part). TRPV4 expression was examined in osteoblasts (B, arrows) and osteoclasts (C, arrowheads) based on immunohistochemistry of the femora (magnification 200 \times). TRPV4 expression in osteocytes was at low level (B, open arrows). Scale bar indicates 20 μ m. D: TRPV4 mRNA expression in cell lines was examined based on RT-PCR. TRPV4 mRNA was observed in MC3T3-E1 osteoblastic cell line. TRPV4 mRNA expression levels in RAW264.7 macrophage cell line were low, but RANKL treatment enhanced the expression levels (** $P < 0.01$). Three wells were used per each group.

expressed in the cells in both osteoblastic and osteoclastic lineages.

Discussion

We identified that TRPV4 is involved in the unloading-induced reduction in bone mass. TRPV4 deficiency suppressed

unloading-induced reduction in bone mass (BV/TV) and bone formation rate (BFR). TRPV4 deficiency also suppressed unloading-induced increase in the number of osteoclasts in primary trabecular bone. These results indicate that TRPV4 is involved in unloading-induced osteopenia through regulation of both bone formation and resorption.

The cells that are responsible for the sensation of mechanical stress have been sought for many years. Osteocytes and osteoblasts are candidate cells to sense mechanical stress and to be involved in the mechanical stress dependent regulation of bone mass. Recent report revealed that targeted ablation of osteocytes in mice resulted in resistant to unloading-induced bone loss (Tatsumi et al., 2007). We observed that TRPV4 protein is expressed in osteoblasts but at least not much in osteocytes in our hand. At this point, we do not exclude a possibility for a low level TRPV4 expression in osteocytes, and thus its function in these cells. Interestingly, TRPV4 is expressed in osteoclasts, a major player of bone resorption. These cells were also reported to be involved in the response to mechanical stress (Kurata et al., 2001). Thus, our identification of TRPV4 to be responsible for unloading-induced bone loss would shed light on the role of this molecule in several types of cells acting in the bone microenvironment.

We previously observed that unloading-induced bone loss was prevented by suppression of sympathetic tone via destruction of ventromedial hypothalamus (Hino et al., 2006) or administration of β blockers (Kondo et al., 2005). In fact, sympathetic tone is involved in bone homeostasis via suppression of bone formation by osteoblasts and activation of resorption by osteoclasts (Takeda et al., 2002; Elefteriou et al., 2005). As TRPV4 was reported to be expressed in sympathetic nerve fibers (Delany et al., 2001), this nervous system could be one of the downstream targets involved in the pathway where TRPV4 deficiency would influence as observed in this paper.

Molecular mechanisms and signaling events before and after calcium influx via TRPV4 have not been fully understood. However, previous reports about TRPV4 and other TRP channels suggested possibility for two mechanisms that could be involved in bone mass regulation by TRPV4. One is its function as a stretch activated channel, and the other is related to signaling through interaction with cytoskeleton molecules (Corey et al., 2004; Maroto et al., 2005). TRPV4 is activated by physical stimuli including fluid shear stress, which leads to calcium influx via stretch and interaction with cytoskeleton (Gao et al., 2003). Fluid flow modulates structures of cytoskeleton in the cells to which TRPV4 is bound (Ramadass et al., 2007). Functional link exists between TRPV4 and cytoskeleton in that disruption of actin microfilaments abolishes calcium influx of TRPV4 (Suzuki et al., 2003a). Loss of mechanical stress in bone affects organization of the actin filaments (Meyers et al., 2005). Thus, TRPV4 deficiency may affect unloading-induced bone loss due to the loss of sensation of mechanical signals being delivered by cytoskeleton.

TRP channels have been reported to be thermosensitive ion channels. These channels include TRPV1, TRPV2, TRPV3, TRPV4, TRPM8, and TRPA1, and each channel exhibits distinct thermal activation threshold (Tominaga and Caterina, 2004). The sensitive temperature range for TRPV4 is relatively narrow (threshold ~ 25 to 34°C) (Watanabe et al., 2002), but these channels may comprehensively respond to diverse temperature. TRPV4 is also reported to serve as a receptor for the high-threshold heat and pressure stimuli in neurons (Caterina et al., 1999; Suzuki et al., 2003b). If analogy to such thermosensitivity could hold true for mechanosensing, several TRP channels might be involved in sensing mechanical stress in bone tissue by sharing their roles on various levels of mechanical stresses. In this case, TRPV4 deficiency may not alter the base line levels of bone mass, if the threshold range for the TRPV4 is not for the levels of stress to bone under

physiologically normal condition (loading) and thus TRPV4 deficient mice only reveal their phenotype upon unloading. In this regards, TRPV4 would be an indispensable mechanosensitive channels in bone in the case of unloading-induced bone loss.

Unloading-induced increase in osteoclast number within primary trabecular regions was not observed in the absence of TRPV4. Osteoclastogenesis is regulated through cell-cell interactions between precursor cells and osteoblasts/stromal cells and TRPV4 is expressed in both osteoclasts and osteoblasts. Thus, cell-cell interaction may be affected by TRPV4 via membrane-bound cytokines. In fact, osteoclastogenesis is controlled by local factors and cytokines including M-CSF and RANKL. However, mRNA expression levels of the cytokines and other marker gene products were not altered by unloading nor the genotype (data not shown). Therefore, we assume that the action point(s) of TRPV4 would be cell autonomous via its regulation of intracellular signaling events including those regulated by intracellular calcium.

The period for the tail suspension was set to 2 weeks in our experiments. Whether the reduced response to tail suspension in the TRPV4 deficient mice would be due to the 2 weeks regimen remains to be elucidated. However, based on the current literatures, tail suspension for 2 weeks was used as a common protocol in many of the published papers (Sakata et al., 2003; Tanaka et al., 2004; Turner et al., 2006). We also observed no major difference in the response in 4 weeks regimen compared to that in the 2 weeks regimen in wild-type mice (data not shown).

In conclusion, TRPV4 deficiency results in loss of mechanosensitivity in bone and suppresses unloading-induced reduction in bone formation and enhancement of bone resorption.

Acknowledgments

This work was supported by the grants-in-aid from the Japanese Ministry of Education (21st Century Center of Excellence (COE) Program for the Frontier Research on Molecular Destruction and Reconstitution of Tooth and Bone, 17012008, 18109011, 18659438, 18123456), grants from Japan Space Forum, JAXA, and ABJS Strategic Research Network Project in Japan Society for Promotion of Science Core to Core Program. We thank R. Kanda, K. Furuya, K. Hayakawa, F. Lopez, N. Sakaguchi at Nagoya University, Y. Hayashida at University of Tokyo, H. Kondo, M. Usui and K. Yumoto for helpful discussion and assistance.

Literature Cited

- Caterina MJ, Rosen TA, Tominaga M, Brake AJ, Julius D. 1999. A capsaicin-receptor homologue with a high threshold for noxious heat. *Nature* 398:436–441.
- Clapham DE. 2003. TRP channels as cellular sensors. *Nature* 426:517–524.
- Corey DP, Garcia-Añoveros J, Holt JR, Kwan KY, Lin SY, Vollrath MA, Amalfitano A, Cheung EL, Derfler BH, Duggan A, Géléoc GS, Gray PA, Hoffman MP, Rehm HL, Tamasauskas D, Zhang DS. 2004. TRPA1 is a candidate for the mechanosensitive transduction channel of vertebrate hair cells. *Nature* 432:723–730.
- Cuajungco MP, Grimm C, Oshima K, D'hoedt D, Nilius B, Mensenkamp AR, Bindels RJ, Plamann M, Heller S. 2006. PACSINs bind to the TRPV4 cation channel. PACSIN 3 modulates the subcellular localization of TRPV4. *J Biol Chem* 281:18753–18762.
- Delany NS, Hurle M, Facer P, Alnadaf T, Plumpton C, Kinghorn I, See CG, Costigan M, Anand P, Woolf CJ, Crowther D, Sanseau P, Tate SN. 2001. Identification and characterization of a novel human vanilloid receptor-like protein, VRL-2. *Physiol Genomics* 4:165–174.
- Ehrlich PJ, Lanyon LE. 2002. Mechanical strain and bone cell function: A review. *Osteoporos Int* 13:688–700.
- Elefteriou F, Ahn JD, Takeda S, Starbuck M, Yang X, Liu X, Kondo H, Richards WG, Bannon TW, Noda M, Clement K, Vaisse C, Karsenty G. 2005. Leptin regulation of bone resorption by the sympathetic nervous system and CART. *Nature* 434:514–520.
- Gao X, Wu L, O'Neil RG. 2003. Temperature-modulated diversity of TRPV4 channel gating: Activation by physical stresses and phorbol ester derivatives through protein kinase C-dependent and -independent pathways. *Journal of Biological Chemistry* 278:27129–27137.
- Genetos DC, Geist DJ, Liu D, Donahue HJ, Duncan RL. 2005. Fluid shear-induced ATP secretion mediates prostaglandin release in MC3T3-E1 osteoblasts. *J Bone Miner Res* 20:41–49.
- Hino K, Nifuji A, Morinobu M, Tsuji K, Ezura Y, Nakashima K, Yamamoto H, Noda M. 2006. Unloading-induced bone loss was suppressed in gold-thioglucose treated mice. *J Cell Biochem* 99:845–852.

- Hsu H, Lacey DL, Dunstan CR, Solovyev I, Colombero A, Timms E, Tan HL, Elliott G, Kelley MJ, Sarosi I, Wang L, Xia XZ, Elliott R, Chiu L, Black T, Scully S, Capparelli C, Morony S, Shimamoto G, Bass MB, Boyle WJ. 1999. Tumor necrosis factor receptor family member RANK mediates osteoclast differentiation and activation induced by osteoprotegerin ligand. *Proc Natl Acad Sci USA* 96:3540–3545.
- Ishijima M, Rittling SR, Yamashita T, Tsuji K, Kurosawa H, Nifuji A, Denhardt DT, Noda M. 2001. Enhancement of osteoclastic bone resorption and suppression of osteoblastic bone formation in response to reduced mechanical stress do not occur in the absence of osteopontin. *J Exp Med* 193:399–404.
- Kizer N, Guo XL, Hruska K. 1997. Reconstitution of stretch-activated cation channels by expression of the alpha-subunit of the epithelial sodium channel cloned from osteoblasts. *Proc Natl Acad Sci USA* 94:1013–1018.
- Kondo H, Nifuji A, Takeda S, Ezura Y, Rittling SR, Denhardt DT, Nakashima K, Karsenty G, Noda M. 2005. Unloading induces osteoblastic cell suppression and osteoclastic cell activation to lead to bone loss via sympathetic nervous system. *J Biol Chem* 280:30192–30200.
- Kurata K, Uemura T, Nemoto A, Tateishi T, Murakami T, Higaki H, Miura H, Iwamoto Y. 2001. Mechanical strain effect on bone-resorbing activity and messenger RNA expressions of marker enzymes in isolated osteoclast culture. *J Bone Miner Res* 16:722–730.
- Lee H, Iida T, Mizuno A, Suzuki M, Caterina MJ. 2005. Altered thermal selection behavior in mice lacking transient receptor potential vanilloid 4. *J Neurosci* 25:1304–1310.
- Liedert A, Kaspar D, Blakytyn R, Claes L, Ignatius A. 2006. Signal transduction pathways involved in mechanotransduction in bone cells. *Biochem Biophys Res Commun* 349:1–5.
- Liedtke W, Friedman JM. 2003. Abnormal osmotic regulation in *trpv4*^{–/–} mice. *Proc Natl Acad Sci USA* 100:13698–13703.
- Liedtke W, Choe Y, Marti-Renom MA, Bell AM, Denis CS, Sali A, Hudspeth AJ, Friedman JM, Heller S. 2000. Vanilloid receptor-related osmotically activated channel (VR-OAC), a candidate vertebrate osmoreceptor. *Cell* 103:525–535.
- Maroto R, Raso A, Wood TG, Kurosky A, Martinac B, Hamill OP. 2005. TRPC1 forms the stretch-activated cation channel in vertebrate cells. *Nat Cell Biol* 7:179–185.
- Meyers VE, Zayzafoon M, Douglas JT, McDonald JM. 2005. RhoA and cytoskeletal disruption mediate reduced osteoblastogenesis and enhanced adipogenesis of human mesenchymal stem cells in modeled microgravity. *J Bone Miner Res* 20:1858–1866.
- Miao D, Bai X, Panda DK, Karaplis AC, Goltzman D, McKee MD. 2004. Cartilage abnormalities are associated with abnormal *Phex* expression and with altered matrix protein and MMP-9 localization in *Hyp* mice. *Bone* 34:638–647.
- Mizuno A, Matsumoto N, Imai M, Suzuki M. 2003. Impaired osmotic sensation in mice lacking TRPV4. *Am J Physiol* 285:C96–C101.
- Morinobu M, Nakamoto T, Hino K, Tsuji K, Shen ZJ, Nakashima K, Nifuji A, Yamamoto H, Hirai H, Noda M. 2005. The nucleocytoplasmic shuttling protein Clz reduces adult bone mass by inhibiting bone morphogenetic protein-induced bone formation. *J Exp Med* 201:961–970.
- Parfitt AM, Drezner MK, Glorieux FH, Kanis JA, Malluche H, Meunier PJ, Ott SM, Recker RR. 1987. Bone histomorphometry: Standardization of nomenclature, symbols, and units. Report of the ASBMR Histomorphometry Nomenclature Committee. *J Bone Miner Res* 2:595–610.
- Pavalko FM, Norvell SM, Burr DB, Turner CH, Duncan RL, Bidwell JP. 2003. A model for mechanotransduction in bone cells: The load-bearing mechanosomes. *J Cell Biochem* 88:104–112.
- Ramadass R, Becker D, Jendrach M, Bereiter-Hahn J. 2007. Spectrally and spatially resolved fluorescence lifetime imaging in living cells: TRPV4-microfilament interactions. *Arch Biochem Biophys* 463:27–36.
- Ramsey IS, Delling M, Clapham DE. 2006. An introduction to TRP channels. *Annu Rev Physiol* 68:619–647.
- Sakata T, Halloran BP, Elalieh HZ, Munson SJ, Rudner L, Venton L, Ginzinger D, Rosen CJ, Bikle DD. 2003. Skeletal unloading induces resistance to insulin-like growth factor I on bone formation. *Bone* 32:669–680.
- Sudo H, Kodama HA, Amagai Y, Yamamoto S, Kasai S. 1983. In vitro differentiation and calcification in a new clonal osteogenic cell line derived from newborn mouse calvaria. *J Cell Biol* 96:191–198.
- Suzuki M, Hirao A, Mizuno A. 2003a. Microtubule-associated [corrected] protein 7 increases the membrane expression of transient receptor potential vanilloid 4 (TRPV4). *J Biol Chem* 278:51448–51453.
- Suzuki M, Mizuno A, Kodaira K, Imai M. 2003b. Impaired pressure sensation in mice lacking TRPV4. *J Biol Chem* 278:22664–22668.
- Takeda S, Eleftheriou F, Levasseur R, Liu X, Zhao L, Parker KL, Armstrong D, Ducey P, Karsenty G. 2002. Leptin regulates bone formation via the sympathetic nervous system. *Cell* 111:305–317.
- Tanaka S, Sakai A, Tanaka M, Otomo H, Okimoto N, Sakata T, Nakamura T. 2004. Skeletal unloading alleviates the anabolic action of intermittent PTH(1–34) in mouse tibia in association with inhibition of PTH-induced increase in c-fos mRNA in bone marrow cells. *J Bone Miner Res* 19:1813–1820.
- Tatsumi S, Ishii K, Amizuka N, Li M, Kobayashi T, Kohno K, Ito M, Takeshita S, Ikeda K. 2007. Targeted ablation of osteocytes induces osteoporosis with defective mechanotransduction. *Cell Metabolism* 5:464–475.
- Todaka H, Taniguchi J, Satoh J, Mizuno A, Suzuki M. 2004. Warm temperature-sensitive transient receptor potential vanilloid 4 (TRPV4) plays an essential role in thermal hyperalgesia. *J Biol Chem* 279:35133–35138.
- Tominaga M, Caterina MJ. 2004. Thermosensation and pain. *J Neurobiol* 61:3–12.
- Turner RT, Lotinun S, Hefferan TE, Morey-Holton E. 2006. Disuse in adult male rats attenuates the bone anabolic response to a therapeutic dose of parathyroid hormone. *J Appl Physiol* 101:881–886.
- Voets T, Nilius B. 2003. TRPs make sense. *J Membr Biol* 192:1–8.
- Vogel V, Sheetz M. 2006. Local force and geometry sensing regulate cell functions. *Nature Rev* 7:265–275.
- Watanabe H, Vriens J, Suh SH, Benham CD, Droogmans G, Nilius B. 2002. Heat-evoked activation of TRPV4 channels in a HEK293 cell expression system and in native mouse aorta endothelial cells. *J Biol Chem* 277:47044–47051.
- Xian CJ, Cool JC, Scherer MA, Macsai CE, Fan C, Covino M, Foster BK. 2007. Cellular mechanisms for methotrexate chemotherapy-induced bone growth defects. *Bone* 41:842–850.
- Xian CJ, Cool JC, Scherer MA, Fan C, Foster BK. 2008. Folic acid attenuates methotrexate chemotherapy-induced damages on bone growth mechanisms and pools of bone marrow stromal cells. *J Cell Physiol* 214:777–785.